Propulsion and Power Research 2012;1(1):64–70

http://ppr.buaa.edu.cn/

Propulsion and Power Research

www.sciencedirect.com

ORIGINAL ARTICLE

Investigation on flow and heat transfer characteristics in rectangular channel with drop-shaped pin fins

Fengming Wang[a], **Jingzhou Zhang**[b,*], **Suofang Wang**[b]

[a]*Research Institute on General Development and Evaluation of Equipment, EAAF of PLA, Beijing 100076, China*
[b]*College of Energy and Power Engineering, Nanjing University of Aeronautics and Astronautics, Nanjing 210016, China*

Received 29 February 2012; accepted 21 September 2012
Available online 20 December 2012

KEYWORDS

Enhanced heat transfer;
Pin fins;
Drop-shaped pin fins;
Pressure loss;
Specific friction loss

Abstract The flow and heat transfer characteristics inside a rectangular channel embedded with pin fins were numerically and experimentally investigated. Several differently shaped pin fins (i.e., circular, elliptical, and drop-shaped) with the same cross-sectional areas were compared in a staggered arrangement. The Reynolds number based on the obstructed section hydraulic diameter (defined as the ratio of the total wetted surface area to the open duct volume available for flow) was varied from 4800 to 8200. The more streamlined drop-shaped pin fins were better at delaying or suppressing separation of the flow passing through them, which decreased the aerodynamic penalty compared to circular pin fins. The heat transfer enhancement of the drop-shaped pin fins was less than that of the circular pin fins. In terms of specific performance parameters, drop-shaped pin fins are a promising alternative configuration to circular pin fins.

1. Introduction

Short pin fin arrays (pin height to pin diameter ratio of less than four) are widely used for turbine blade trailing edges, compact heat exchangers, electronics heat sinks, and other applications that require high heat flux removal rates. These pin fins inside the flow channel promote turbulence to enhance the convective heat transfer level, even if the pin fins are made of material with low heat conductivity [1]. Inline and staggered

*Corresponding author: Tel.: +86 25 84895909.
E-mail address: zhangjz@nuaa.edu.cn (Jingzhou Zhang)

Peer review under responsibility of National Laboratory for Aeronautics and Astronautics, China.

Production and hosting by Elsevier

2212-540X © 2012 National Laboratory for Aeronautics and Astronautics. Production and hosting by Elsevier B.V. All rights reserved.
http://dx.doi.org/10.1016/j.jppr.2012.10.003

Nomenclature

A_f	wetted surface area (unit: m^2)
A_p	pin section area (unit: m^2)
B	rectangular duct width (unit: m)
c_p	heat capacity (unit: $J/(kg \cdot K)$)
D_h	hydraulic diameter (unit: m)
f	pressure loss coefficient
h	convective heat transfer coefficient (unit: $W/(m^2 \cdot K)$)
H	rectangular duct height (unit: m)
L	length of pin fins array in x-direction (unit: m)
L_p	pin circumference length (unit: m)
m	flow mass rate (unit: kg/s)
N	number of pin fins
Nu	Nusselt number
P	pressure (unit: Pa)
q	density of heat flow rate (unit: W/m^2)
Re	Reynolds number
T	thermodynamic temperature (unit: K)
u	velocity (unit: m/s)
V_f	fluid volume inside pin fins array region (unit: m^3)
x	streamwise direction
x_n	streamwise pitch
y_n	spanwise pitch
y	spanwise direction
z	z-direction

Greek letters

v	kinematic viscosity (unit: $Pa \cdot s$)
λ	thermal conductivity (unit: $W/(m \cdot K)$)
ξ	specific performance parameter

Subscripts

av	average
f	fluid
in	inlet
max	maximum
out	outlet
w	wall

arrays of short circular pin fins are the most common configurations used in these applications, and many studies have been conducted on this topic. VanFossen [2] investigated the heat transfer coefficients for staggered arrays of short pin fins. Metzger et al. [3] studied the developing heat transfer in rectangular ducts with staggered arrays of short pin fins. Chyu and Goldstein [4] studied the influence of an array of wall-mounted cylinders on the heat transfer from flat surfaces by using the and pressure drop of the common pin fins revealed that the diameter, height, and arrangement of pin fins are the main factors influencing heat transfer enhancement and pressure loss.

Circular pin fins have the disadvantage of early flow separation over the fin, which increases the total pressure drop across the duct. To improve the integrative performance of the flow and heat transfer inside a rectangular channel equipped with pin fins, a particular area of interest is using different pin shapes that can delay flow separation. Pin fins with oblong cross sections were investigated by Metzger et al. [5] for various pin orientations with respect to the main flow. Their results indicated that the use of oblong-shaped pin fins increases endwall heat transfer but also increases the aerodynamic penalty compared to circular pin fins when the main flow direction deviates from the direction of the major axis of the oblong pin fin. When the main flow approaches the pin fins with no direction deviation, the pressure loss levels become lower than that of circular pin fins. Chyu et al. [6] investigated the heat transfer and pressure loss characteristics of cubic- and diamond-shaped pin fin arrays for both inline and staggered configurations. They found that cubic pin fin arrays produced the highest heat transfer rates, and the diamond pin fin array induced the greatest pressure loss. Li et al. [7] investigated elliptical pin fin arrays for Reynolds numbers ranging from 900 to 9000. The major and minor axes of the elliptical pin fins were chosen such that the pin fin circumferences were equal to the corresponding circular pin fins. The experimental results showed that the heat transfer inside a channel embedded with elliptic pin fins was somewhat higher than that with circular pin fins, whereas the resistance of the former was much lower than that of the latter. Uzol and Camci [8,9] also conducted similar experiments with two different types of elliptical pin fins, but their results were in contrast to those of Li et al. [7] with regard to heat transfer enhancement. Circular pin fin arrays enhance wall heat transfer by about 25%–30% more than elliptical pin fin arrays on average.

In terms of reducing the pressure drop across the pin fin array, streamlined drops may be the best shape for the pin fin cross section. Chen et al. [10] conducted an experiment on the internal flow and heat transfer with drop-shaped pin fins. Their results indicated that drop-shaped pin fins yield a considerable improvement in heat transfer compared to circular pin fins for the same pressure drop characteristics. Note that this comparison was based on the windward area condition. This means that the wetted surface area of the drop-shaped pins increased in comparison to the circular pins.

The objective of the current study was to increase an understanding of the flow and heat transfer characteristics in a rectangular channel embedded with staggered drop-shaped pin fins. Three types of drop shapes were designed for computational and experimental investigation, and a comparison with differently shaped pins (e.g. circular and elliptical) was also carried out. All the pin fins had the

same cross-sectional areas and were arranged in the rectangular channel with no main flow direction deviation.

2. Experiment scheme

2.1. Experimental setup

Figure 1(a) shows the experimental setup, which comprises a compressor, a chamber with a converging nozzle, a hydrodynamic developing section, a test section and an exit section. Compressed air (pressure of 0.12 MPa and temperature of 30 °C) is forced to enter the chamber, and the mass flow rate is measured by a standard orifice plate flow metre located in the flow metering supply, upstream of the chamber. The hydrodynamic developing section is 500 mm long to ensure a fully developed flow up to a Reynolds number of 10,000. The rectangular cross section has a width of 120 mm and a height of 10 mm to be consistent with the test section. The test section is made of an 8 mm thick transparent plate. It has a length of 130 mm to house six rows of pin fins set up with axes perpendicular to the direction of flow in a fixed staggered array (Figure 1(b)). The streamwise and spanwise pitches are $x_n = 12$ mm and $y_n = 24$ mm, respectively. The pin fins are made of stainless steel. Two thin heater sheets with uniform resistance (100 mm wide, 100 mm long, and 0.01 mm thick) covert each inner surface of two sidewalls. The pin fins are installed to be in contact with the heater sheet, with a thin

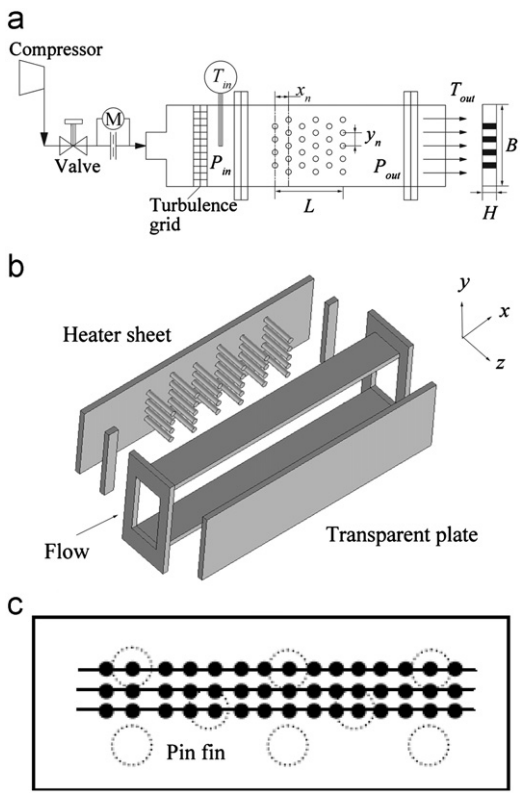

Figure 1 Schematic diagram of experimental facility. (a) Layout of test system, (b) test section and (c) arrangement of thermocouples.

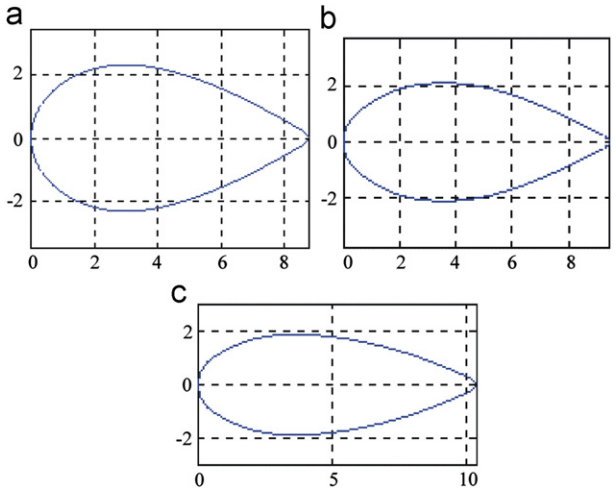

Figure 2 Cross-sectional geometries of drop-shaped pins. (a) Drop-A, (b) drop-B and (c) drop-C.

mica sheet acting as an interface. Each heater sheet is equipped with two electrodes to provide controllable uniform heat flux. To reduce heat losses from the heater to the outside, the test section is insulated by a 20 mm thick asbestos shroud. The exit section length is 400 mm to allow free expansion of the flow and is insulated to reduce heat losses. Two pressure taps are at the inlet and outlet of the test section to measure the pressure drop inside the test section.

Forty-five thermocouples are mounted at the back face of the heater sheet to measure the temperature distribution; because the Biot number ($Bi = h\delta/\lambda_s$, where δ and λ_s are the thickness and thermal conductivity, respectively, of the heater sheet) was much less than unity, the temperature could be considered to be practically uniform across the sheet thickness. These thermocouples are aligned in three rows, as shown in Figure 1(c).

2.2. Pin geometry

A circular pin, an elliptical pin, and three drop-shaped pins were designed and tested in the current study. The pins all have the same cross-sectional area. The diameter of the circular pin is 6 mm. The elliptical pin has a minor axis length of 2.12 mm and major axis length of 4.24 mm. Figure 2 shows three drop-shaped pins: drop-A, drop-B, and drop-C. Their lengths are 8.5, 9.2, and 10.1 mm, respectively, and the corresponding large widths are 4.6, 4.2 and 3.8 mm, respectively.

3. Computation scheme

3.1. Computational domain

The physical model was built according to the experimental model. It comprises an inlet section, test

section, and exit section. The fluid and pin fins were modelled as a 'conjugated' computational domain. To minimise the computational requirements and time, only one-fourth of the cross section in the streamwise direction was modelled, and two symmetry planes were applied to the domain boundary.

The boundaries are summarised as follows:

Inlet: The flow temperature (T_{in}) was set to 303 K to be consistent with the experimental case, and the inlet velocity (u_{in}) was determined by the chosen Reynolds number. A turbulence intensity of 1% and turbulence length scale of 3% for the inlet height were used.

Walls: The no-slip condition was applied to all the solid walls. An adiabatic thermal condition was applied to the endwalls, and a constant heat flux condition ($q=10{,}000\ \mathrm{W/m^2}$) was applied to the heated sidewalls.

Symmetry planes: The symmetry planes were assumed to be modelled with zero heat flux. The mid-height plane was given zero velocity in the z direction ($u_z=0$), and the mid-width plane was given a zero velocity in the y direction ($u_y=0$); this prevented the flow from crossing the boundary yet allowed a velocity profile to develop.

Pins: The pin was treated as a solid volume with a constant thermal conductivity of $15\ \mathrm{W/(m\cdot K)}$. The pins were therefore assumed to be conjugated with the fluid. The no-slip condition was applied to the pin surfaces.

Outlet: The derivations of all the variables along the streamwise direction were set to zero.

3.2. Numerical mesh

An unstructured grid system was employed in this study to meet the complex internal configuration of a channel embedded with pin fin arrays. Meshing was refined in some critical areas to ensure coverage for satisfactory resolution: near the no-slip walls where velocity and temperature gradients were expected to be high and between the pins to capture the flow acceleration due to the decrease in cross-sectional area. Approximately 650,000 computational grids were involved in the entire computational domain and about 2000 grids in each pin fin. A run was considered to be grid-independent, if the overall heat transfer rate difference between the two remained below 2%.

3.3. Computational approach

Three-dimensional numerical simulation was performed using Fluent-CFD software. First-order upwind was selected for the discreteness of the governing equations, and the standard k–ε turbulence model was applied. It was necessary to control the speed of calculation through under-relaxation. Convergence was considered to be achieved when both of the following criteria were met: (a) a reduction in all residuals of five orders in magnitude and (b) no observable change in the predicted surface temperature for an additional 50 iterations. More details on these solvers can be found in the ANSYS Fluent Software User's Guide [11].

4. Parameters and data treatment

The hydraulic diameter is defined as the ratio of the open duct volume available for flow to the total wetted surface area inside the pin fin array region. This ratio is the most appropriate characteristic length because it is representative of the different configurations investigated in this study and captures the influence of all the length scales in the problem.

$$D_h = 4V_f/A_f \tag{1}$$

where V_f is the total fluid volume inside the pin fins array region. A_f is the wetted surface area, which is defined as the total convective heat transfer area in contact with the coolant fluid. The total convective heat transfer area includes the wall and pin areas in contact with the fluid.

For a rectangular duct with width B and height H, pin with section area A_P and circumference length L_p, number of pin fins N, and length of pin fin array in the streamwise direction L,

$$V_f = BHL - NA_PH$$

$$A_f = 2(B+H)L + N\left(L_pH - 2A_P\right)$$

The hydraulic diameters for different pins in the present study are summarised in Table 1.

The Reynolds number is defined based on the hydraulic diameter.

$$Re = u_{max}D_h/v \tag{2}$$

where u_{max} is the maximum flow velocity in a channel embedded with a pin fin array and v is the kinematic viscosity of the coolant.

The local and average convective heat transfer coefficients are defined as

$$h = \frac{q}{T_w - T_f}, \quad h_{av} = \frac{q}{T_{w,av} - T_{f,av}} \tag{3}$$

where q is the heat flux forcing on the heated surface; T_w is the local temperature at the endwall; $T_{w,av}$ is the average temperature at the endwall; T_f is the local section-averaged temperature of the coolant flow, which is calculated by assuming that it varies linearly along the streamwise direction; and $T_{f,av}$ is the total average

Table 1 Hydraulic diameters (unit: mm).

Shape	Circular	Elliptical	Drop-A	Drop-B	Drop-C
D_h	14.1	13.8	13.7	13.6	13.3

temperature of the coolant flow, which is taken as the arithmetic average of the inlet temperature ($T_{f,in}$) and outlet temperature ($T_{f,out}$).

The outlet temperature was calculated as below using an energy balance across the ends of the test section.

$$T_{f,out} = T_{f,in} + \frac{2qA_{heater}}{mc_p}$$

where m is the flow mass rate, c_p is the specific heat of the coolant, and A_{heater} is the heated surface area on each sidewall.

The local and average Nusselt numbers are defined based on the hydraulic diameter

$$Nu = \frac{hD_h}{\lambda}, \quad Nu_{av} = \frac{h_{av}D_h}{\lambda} \tag{4}$$

where λ is the conductivity of the coolant.

The total pressure loss coefficient or friction coefficient is defined as

$$f = \frac{P_{in} - P_{out}}{(1/2)\rho u_{in}^2} \tag{5}$$

where P_{in} and P_{out} are the total pressures at the inlet and outlet sections, respectively.

A specific performance parameter that considers both heat transfer enhancement and pressure loss was introduced in [8]

$$\xi = \frac{f}{Nu_{av}} \tag{6}$$

5. Results and analysis

5.1. Flow characteristics

Figure 3 shows the detailed local vorticity distributions on the mid-height plane of the flow channel for different pins. Two vortical structures dominated the vorticity distribution: horseshoe and wake vortices. The occurrence of these vortical structures depends on the interaction of the primary flow and pin fins. Horseshoes are formed in the flow around a blunt body and roll up at the pin rim. Wakes are induced by flow separation when the windward flow is exposed to a blunt body and manifests near the trailing edge of a pin. The horseshoe is a considerably smaller structure with a negligible effect on the aerodynamic penalty compared to wake vortices. As expected, the drop-shaped pin yields a reduced aerodynamic penalty compared to circular pins owing to its considerably weaker flow separation.

Figure 4 shows the pressure loss coefficient versus the Reynolds number (based on the hydraulic diameter) for the channel with different pin fin arrays. Although there was a distinct difference between the computational and experimental results, the varying trends in the pressure loss coefficient versus the Reynolds number were in good agreement.

At Reynolds numbers of 4800–8200, the elliptical and drop-A pin fins seem to show a decrease of about 36% in the pressure loss coefficient relative to the pressure loss coefficient of the circular pins. As the tail length of the drop was increased, the pressure loss coefficient decreased owing to flow separation suppression, which reduced the flow drag. The drop-B and drop-C pins showed decreases of about 45% and 55%, respectively, in pressure loss coefficient relative to that of the circular pin. This comparison was made using experimental data. As expected, the more streamlined drop-shaped pins delayed or suppressed separation when the flow passed through them, which is the main mechanism for yielding a considerable reduction in aerodynamic penalty. Another reason for the decrease in the pressure loss coefficient was that the windward blockage under the drop-shaped pin fin arrays was less compared to the windward blockage under circular pins; this forced the flow to follow a weakly twisted path around the pins and resulted in a decrease in the pressure drop.

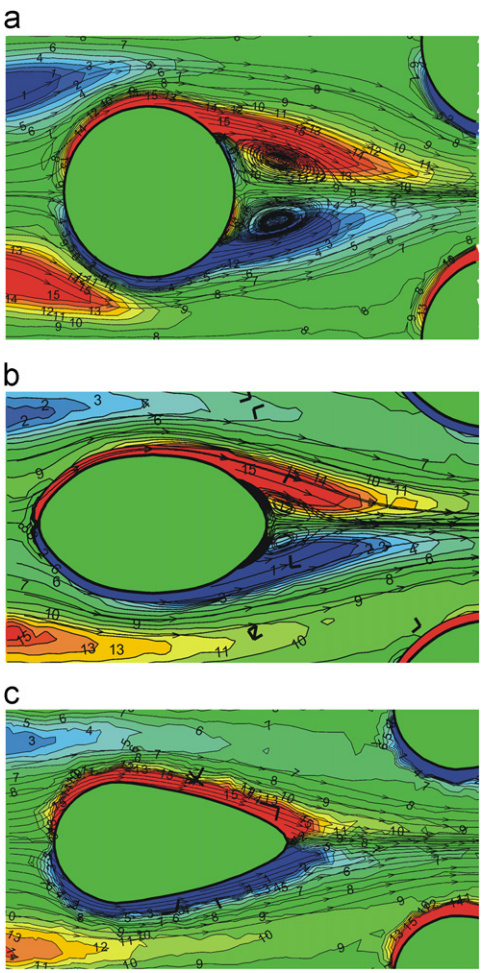

Figure 3 Local vorticity contours for different pins (from computation). (a) Circular pin, (b) elliptical pin and (c) drop-shaped pin.

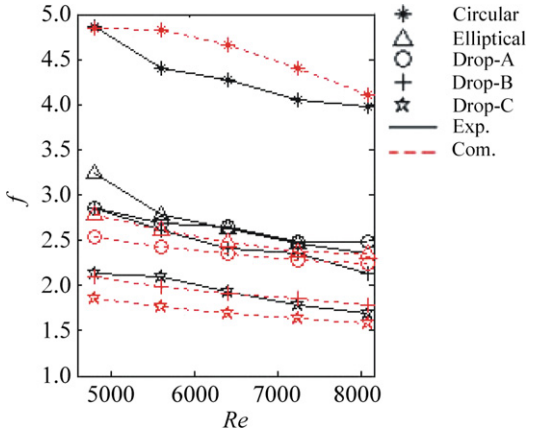

Figure 4 Pressure loss coefficient versus *Re* number.

5.2. Heat transfer characteristics

Figure 5 shows the computational results of local Nusselt number distributions at the heated wall with different types of pin fin arrays when $Re=6400$.

The local heat transfer was significantly enhanced in the regions near the pin fin circumferences for all the cases. In the rear wakes of pin fins, the local convective heat transfer capacities also remained at higher levels. These features may be attributed to the actions of the horseshoe and wake vortices. As noted in section 5.1, circular pins have a wider separation region in the trailing edge of the pin. Consequently, circular pins seemed to have the strongest convective heat transfer intensity among the five cases in the current study. In addition, the windward blockage by a circular pin fin array was maximal for all cases; the flow was forced to follow a more twisted path around the pins, which decreased the pressure drop.

Figure 6 shows the average Nusselt number versus the Reynolds number (based on the hydraulic diameter) for the channel with different pin fin arrays. Although there was a greater relative error of 10%–20% between the computational and experimental results, the relation of the convective heat transfer capacities versus the pin shapes agreed well.

At Reynolds numbers of 4800–8200, the elliptical pin fins seemed to decrease the average Nusselt number by about 20% relative to the circular pins. For the drop-shaped pin fins, the reduction in average Nusselt number relative to that for the circular pin was about 24% for drop-A, 26% for drop-B, and 27% for drop-C. The obtained results agree with the conclusions of Uzol and Camci [8,9]: greater heat transfer enhancement is obtained by paying a greater aerodynamic penalty.

5.3. Specific friction loss

The heat transfer behaviour alone does not provide a complete evaluation of heat exchanger performance.

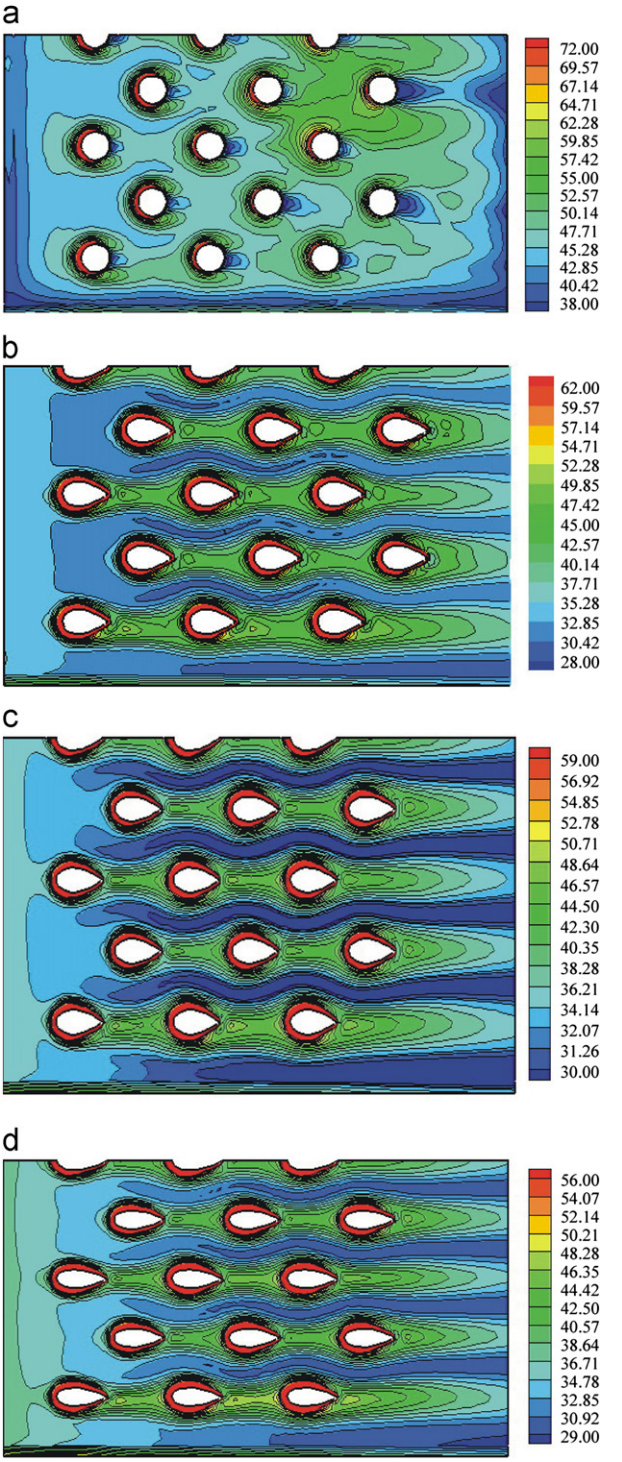

Figure 5 Local *Nu* number distributions (from computation). (a) Circular pin fins, (b) drop-A pin fins, (c) drop-B pin fins and (d) drop-C pin fins.

The increase in pressure drop, which is a measure of the energy required by the system, must be weighed against the improvement in heat transfer for each pin fin configuration. This optimisation process is critical for improving energy efficiency and comparing the contrast between heat exchanger gains and losses. The specific

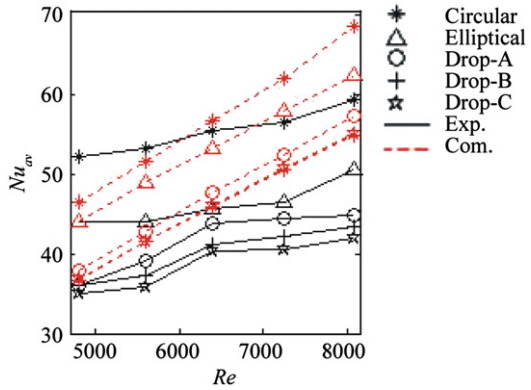

Figure 6 Average *Nu* numbers versus *Re* number.

Table 2 Specific friction losses ($Re=6400$).

Shape	Circular	Elliptical	Drop-A	Drop-B	Drop-C
Exp.	0.072	0.053	0.047	0.041	0.038
Com.	0.077	0.047	0.049	0.042	0.037

friction loss (as seen in Eq. (6)) was adopted to evaluate the optimisation of the pin shapes.

The specific friction losses for different pins in the case of $Re=6400$ are summarised in Table 2. The specific friction loss of drop-shaped pin fins was lower than that of elliptical and circular pin fins, which indicates that the drop-shaped pin is more advantageous than the others.

6. Conclusions

This paper summarises computational and experimental results for research on the flow and heat transfer process of a rectangular channel embedded with staggered pin fins.

(1) The more streamlined drop-shaped pin fins are better at delaying or suppressing separation when a flow passes through them, which reduces the aerodynamic penalty compared to circular pin fins. The drop-B and drop-C pins showed decreases of about 45% and 55%, respectively, in pressure loss coefficient relative to that in the circular pin.

(2) The heat transfer enhancement of drop-shaped pin fins is weaker than that of circular pin fins. The reduction in average Nusselt number between the drop-shaped and circular pins was about 24% for drop-A, 26% for drop-B, and 27% for drop-C.

(3) For the specific performance, the specific friction loss in drop-shaped pin fins was lower than that of elliptical and circular pin fins, which indicates that the drop-shaped pin is more advantageous than the others. Thus, drop-shaped pin fins are a promising alternative configuration to circular pin fins.

Acknowledgements

The authors gratefully acknowledge the financial support received from the National Natural Science Foundation of China (Grant no. 51276090) for this project.

References

[1] J. Armstrong, D. Winstanley, A review of staggered array pin fin heat transfer for turbine cooling applications, ASME Journal of Turbomachinery 110 (1) (1988) 94–103.

[2] G.J. VanFossen, Heat transfer coefficients for staggered arrays of short pin fins, Journal of Engineering for Power 104 (2) (1982) 268–274.

[3] D.E. Metzger, R.A. Berry, J.P. Bronson, Developing heat transfer in rectangular ducts with staggered arrays of short pin fins, Journal of Heat Transfer 104 (1982) 700–706.

[4] M.K. Chyu, R.J. Goldstein, Influence of an array of wall-mounted cylinders on the mass transfer from a flat surface, International Journal of Heat Mass Transfer 34 (9) (1991) 2175–2186.

[5] D.E. Metzger, C.S. Fan, S.W. Haley, Effects of pin shape and array orientation on heat transfer and pressure loss in pin fin arrays, Journal of Engineering for Gas Turbines and Power 106 (1984) 252–257.

[6] M.K. Chyu, Y.C. Hsing, V. Natarajan, Convective heat transfer of cubic pin fin arrays in a narrow channel, ASME Journal of Turbomachinery 120 (2) (1998) 362–367.

[7] Q. Li, Z. Chen, U. Flechtner, H.J. Warnecke, Heat transfer and pressure drop characteristics in rectangular channels with elliptic pin fins, International Journal of Heat and Fluid Flow 19 (3) (1998) 245–250.

[8] Q. Uzol, C. Camci, Elliptical pin fins as an alternative to circular pin fins for gas turbine blade cooling applications, part 1: endwall heat transfer and total pressure loss characteristics, ASME Paper 2001-GT-0180, 2001.

[9] Q. Uzol, C. Camci, Heat transfer, pressure loss and flow field measurements downstream of staggered two-row circular and elliptical pin fin arrays, ASME Journal of Heat Transfer 127 (5) (2005) 458–471.

[10] Z. Chen, Q. Li, D. Meier, H.J. Warnecke, Convective heat transfer and pressure loss in rectangular ducts with drop-shaped pin fins, Heat and Mass Transfer 33 (3) (1997) 219–224.

[11] ANSYS Inc., ANSYS Fluent v12.0 Software User's Gide, Lebanon, NH, 2009.